Journal of Power Sources 196 (2011) 5811–5816

Contents lists available at ScienceDirect

Journal of Power Sources

journal homepage: www.elsevier.com/locate/jpowsour

Investigations of a platinum–ruthenium/carbon nanotube catalyst formed by a two-step spontaneous deposition method

Wei-Chin Chang*, Minh Toan Nguyen

Department of Mechanical Engineering, Southern Taiwan University, 1 Nantai Street, Yungkang District, Tainan City, 710, Taiwan

ARTICLE INFO

Article history:
Received 2 March 2011
Accepted 7 March 2011
Available online 11 March 2011

Keywords:
Bimetal catalyst
Carbon nanotube
Spontaneous deposition
Fuel cell

ABSTRACT

Platinum (Pt) is a popular catalyst for hydrogen oxidation on the anode side of solid polymer fuel cells (SPFC). It increases the electrode activity, which catalyzes the reaction of the fuel cell. There are two methods commonly used to produce hydrogen for SPFC: fuel reforming and methanol decomposition. Both of these methods produce carbon monoxide, which is considered to be a poison for SPFC because it deactivates Pt easily. Adding ruthenium (Ru) to a Pt catalyst is an efficient way to improve the inhibition of carbon monoxide (CO) formation and reduce the Pt loading requirement.

This study introduces a method to synthesize a bimetal catalyst that is suitable for SPFC. To improve the electrocatalyst activity, a new process with two spontaneous deposition steps is adopted. In the first step, Ru is deposited on the wall of carbon nanotubes (CNTs) to obtain Ru/CNTs. Pt is then added in the second deposition step to form Pt–Ru/CNTs. The morphology and microstructure of catalysts are characterized with microscopes, and the performance of membrane electrode assembly is evaluated by cyclic voltammetry method. Experimental results have proved that even with a lower Pt loading, this home-brewed bimetal catalyst performs a compatible electrocatalytic activity, and is capable of resisting attack from CO when a syngas (H_2 + 20 ppm CO) is provided.

1. Introduction

Pt is a commonly used catalyst for hydrogen (H_2) oxidation and oxygen (O_2) reduction in electrochemical reaction of the low-temperature fuel cell, which is also referred to as the solid polymer fuel cell. SPFC is considered to be an alternative power source for portable electronic devices and transportation vehicles. One kind of SPFC, a proton exchange membrane fuel cell (PEMFC) prefers pure H_2 fuel. H_2 requires storage space unless it is highly pressurized, which raises a safety issue because it creates a bursting potential. Fuel reforming is a popular method to generate H_2 locally from hydrogen-rich liquid or gaseous fuels, and it is possible to save the required space for H_2 storage. The problem with reforming fuel is the concomitant product CO from the production process, which can poison Pt easily, especially at low temperature (less than 150 °C) [1]. Similar CO production behavior also occurs with another type of SPFC, the direct methanol fuel cell (DMFC), during the decomposition of methanol fuel.

The water–gas shift reaction has been considered a simple way to convert CO into carbon dioxide (CO_2) in industry, but it is difficult to remove CO entirely from the reformate. Even as little as 10 ppm of CO in the feed gas can stop the electrochemical activity of Pt [2]. The poisoning problem can be alleviated by increasing the operating temperature of the fuel cell [3]. However, this type of electrolyte is still not commercially available. Schmidt et al. [4] proposed a solution by bleeding oxidant into the fuel. A small amount of O_2 or oxygen-evolving compound (H_2O_2) was added into the fuel to oxidize the CO, but the presence of oxidant led to a decrease in fuel efficiency and raised a safety problem.

The combination of Pt with another metal catalyst can improve the electrocatalytic activity and protect Pt from poisoning by CO. In the experiment of Ham et al. [5], a mesoporous tungsten carbide of WC-phase was used as the substrate to form a Pt/WC catalyst for anode of PEMFC. Compared with the Pt/C catalyst, the Pt/WC catalyst showed an improved ability to resist CO poisoning. In similar studies, Sn, Os, Co, Mo, Nb and Ta have all been proposed to alloy with Pt [6–8]. Moreover, ternary catalysts, such as PtRuMo [9], PtRuNi [10], Pt–Ru–WC and Pt–Ru–Co [11], were also introduced to PEMFC to gain a more CO-tolerant behavior.

In comparison with other metal catalysts, Ru is the most suitable to alloy with Pt to form an anode catalyst for DMFC [12]. With similar physical and chemical properties to Pt, Ru can easily become a catalyst or co-catalyst material in Pt–Ru alloys to oxidize CO or methanol. The tolerance level of Pt to CO is increased by the presence of Ru, which can be ascribed to two mechanisms: the first is a "bifunctional mechanism", wherein the role of Ru is to provide adsorbed oxygen-containing species to oxidize CO that blocks Pt on the surface of the catalyst; the second is the "ligand

* Corresponding author. Tel.: +886 932 815246; fax: +886 6 2425092.
E-mail address: wcchang@mail.stut.edu.tw (W.-C. Chang).

0378-7753/$ – see front matter © 2011 Elsevier B.V. All rights reserved.
doi:10.1016/j.jpowsour.2011.03.012

effect", in which Ru weakens the Pt–CO bonding [13] to remove CO easily.

To increase the contact surface and reduce the requirement of catalyst loading, Pt and Ru are synthesized at the nanoscale level. By dispersing the metal catalyst on a conductive support, such as carbon powder or a carbon nanotube, the agglomeration of metal particles can be avoided [14]. In some cases, the presence of support also improves the activity of electrocatalysts through the interaction between the metal and the support.

The carbon-supported catalysts can be prepared either by impregnation or ion-exchange methods. These processes facilitate the access of catalysts to the carbon supports and higher catalyst dispersions. The carbon nanotube (CNT) is an ideal material to be used as the substrate for supporting nano-sized metallic particles because it exhibits extraordinary properties, such as high electronic conductivity, chemical stability, inertness and high surface area [15,16]. Carmo et al. [15] produced Pt–Ru/CNT using an impregnation method. Chi et al. [17] concluded that a higher catalyst activity can be obtained by a multiple impregnation process. However, considering the cost, they only added a small amount of CNT to Pt–Ru/C. Yoo et al. [18] said the flat interface between CNTs and Pt–Ru can improve the activity of metal catalysts. On the anode side of DMFC, the oxidation potential of CO is reduced due to the presence of CNT. Instead of using bimetal catalyst, Tanaka et al. [19] added O_2 into an H_2 stream and successfully oxidized 2000 ppm of CO in H_2 with only the Pt/CNT catalyst. This result also revealed the advantage of using CNT as a support catalyst for SPFC.

There are two types of CNTs: the single-walled carbon nanotubes (SWCNTs) and the multi-walled carbon nanotubes (MWCNTs). Wang et al. [20] investigated the electrochemical corrosion behaviors of SWCNTs and MWCNTs. They concluded that a MWCNT is more electrochemically stable than a SWCNT, which makes the MWCNT a proper material for PEMFC. A similar remark was also made by Batra and Sears [21]. Moreover, SWCNT is more expensive than MWCNT, which makes MWCNT a favored material for the support substrate of the Pt–Ru catalyst.

2. Synthesis methods of CNT-supported bimetal catalyst

2.1. General methods

Catalysts for chemical reactions are usually formed by two, three or more noble metals. This type of catalyst is well known for higher catalytic activity than a single metal [22]. Pt–Ru alloys can be prepared by several methods. Most approaches use pure Pt as a substrate and modify it by depositing Ru from the gas phase, aqueous phase or a non-aqueous liquid phase. The method of depositing Ru on Pt influences the morphology and electrocatalytic characteristics of the alloy surface.

There are many methods for depositing Pt on Ru, which include spontaneous deposition [23], forced deposition [24], electrodeposition [25], physical vapor deposition [26], chemical vapor deposition [27] and deposition in non-aqueous solvents [28,29]. Of these methods, spontaneous deposition provides a convenient way to synthesize the Pt–Ru alloy, whereas others require complex materials or expensive instruments to deposit metal onto the substrate. The work presented in this paper is a new method conducted by two consecutive spontaneous deposition processes to synthesize the Pt–Ru/CNT catalyst.

2.2. Two spontaneous deposition steps method

The process of spontaneous deposition proceeds when a clean noble metal surface is in contact with a solution of another noble metal cation. The formed chemisorbed species can readily be reduced to metal or metal oxide islands [30]. The deposition can be completed without applying external potential or adding any reducing agent, and no special attention is required during the procedures [29]. Additionally, this process can be repeated to obtain higher coverage of the desired metal catalyst.

In this study, Ru is spontaneously deposited on CNT, and the product is used as a substrate for Pt deposition. Pt–Ru/CNT catalysts are obtained at the nano size, and Pt exposes a larger surface area that is uncovered by other metal, which will help the gas fuel to contact the Pt easily in the fuel cell application.

3. Experiments

3.1. The first deposition step

CNT is a chemically inert substance; it is necessary to activate the surface before using it as a substrate for dispersion of metallic catalysts. A purification treatment was done first. Because of the porous structure, CNTs usually hold a relatively small amount of chemically bonded heteroatoms (mainly O_2, H_2, and N_2) [31]. CNTs were heated from room temperature to 300 °C and held at this temperature for 3 h. During this pyrolysis process, heteroatoms were released as volatile gaseous products. CNTs were then treated in hydrochloric acid at 70 °C for another 12 h to dissolve other metals. Next, the prepared CNTs were added into the Ruthenium Chloride ($RuCl_3$) solution and stirred vigorously for 2 h at room temperature. Then NaOH was added as a neutralizing agent to remove the remaining hydrogen ions from CNT. The solution was centrifuged and washed with deionized water to remove undesired ions. In the end, the slurry of Ru/CNTs catalyst was dried and stored for later use.

3.2. The second deposition step

To further disperse Pt on the Ru nanoparticles, Ru/CNTs were reduced in the H_2 gas. A specially designed flask imitated from the work of Kuk and Wieckowski [32] was used and immersed in the hot silicone oil. The specimen of dry Ru/CNTs was placed into the flask, and the temperature increased from room temperature to 220 °C with argon gas. When the temperature inside the flask reached to 200 °C, H_2 gas was introduced at the rate of 10 sccm for 3 h. After the reduction process, the specimen was cooled down to the room temperature with argon gas to isolate Ru/CNTs from the ambient air. The specimen was submerged in purified water until the temperature was 25 °C to protect the catalyst surface from oxidation. The wet catalysts were mixed and stirred with the desired amount of hydrogen hexachloroplatinate (IV) hexahydrate ($H_2PtCl_6{\cdot}6H_2O$) and 0.1 M H_2SO_4. After a centrifuging and drying processes, Pt–Ru/CNTs were obtained.

3.3. Catalysts characterization

3.3.1. Physicochemical characters

A Philips Tecnai G2 F20 FEG-TEM operated at 200 kV was used to conduct the measurements of TEM and EDX. The samples were prepared by suspending the catalyst powder in the isopropyl alcohol solution. A drop of solution was then deposited onto a copper grid and subsequently dried. A Hitachi S-300 SEM was used to image the catalyst surface to explore the topography, composition and other properties of the catalysts.

3.3.2. Electrochemical characters

Electrochemical investigations of Pt–Ru/CNTs and Pt–Ru/C black (E-TEK) electrocatalysts were performed by using a thin-film rotating disk electrode. Cyclic voltammetry was carried out in a

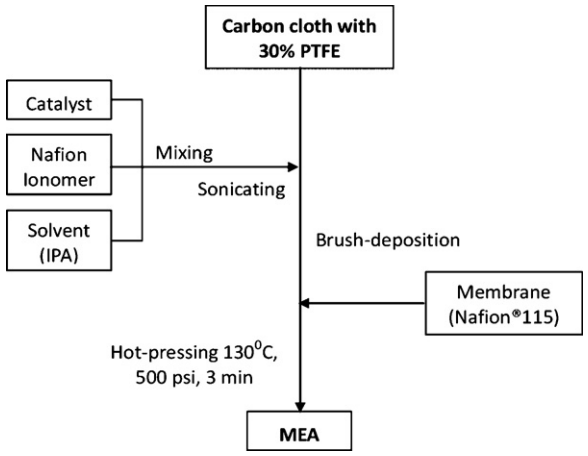

Fig. 1. The procedure of fabricating a membrane electrode assembly.

conventional three-electrode cell, the thin-film electrode was prepared as the working electrode, platinum wire was the counter electrode and silver/silver chloride (Ag/AgCl) was the reference electrode. The working electrode (0.1256 cm^2 of geometric area) was inserted in a polytetrafluoroethylene (PTFE) specimen holder, which allowed the active reaction layer of electrode to expose to the electrolyte. The cell was tested by a PARSTAT 2263 potentiostat interfaced via GPIB to a personal computer. In the preparation of a working electrode, 10 mg of catalysts were dispersed in a mixture containing 56 μl of Nafion solution (5 wt.%), 1 ml isopropyl alcohol and 3.5 ml water. This mixture was stirred for 30 min by ultrasonicating to obtain an ink-like slurry of the catalyst particles. 15 μl of slurry was dropped onto the glassy carbon disk and allowed to dry off at 80 °C for 2 min. 10 μl of Nafion solution (5 wt.%) was spread on the catalyst layer and dried in the oven at 80 °C for 5 min. The Nafion solution functioned as a protective layer to prevent the catalyst from dissolving into the electrolyte. For all experiments, the working electrode was rotated at 500 rpm. The stable voltammetry profiles in the potential region (from 0 to 0.8 V) were recorded after 3 scanning cycles.

3.4. Fuel cell test

3.4.1. Preparation of the membrane electrode assembly

A Nafion 115 membrane was cleaned in the deionized water for 12 h to ensure that it was in the protonic form. To form the catalyst layer of the electrode, a homogeneous suspension was prepared. A mixture of isopropyl alcohol and Nafion ionomer (5 wt.% of Nafion) with the desired amounts of catalyst was prepared by stirring in an ultrasonic bath at room temperature for 15 min. The amount of Nafion ionomer is 30 wt.% of the catalyst. The resulting ink was brush-deposited on the surface of the gas diffusion layer (GDL), which was a piece of carbon cloth coated with PTFE.

A Nafion 115 membrane was sandwiched between two prepared carbon cloths (anode and cathode). This three-piece structure was pressed together at a pressure of 500 psi at 130 °C for 3 min. Fig. 1 shows the forming process of the membrane electrodes assembly (MEA). Three different MEAs were made as described in Table 1 for the performance tests.

3.4.2. Measurement of single fuel cell performance

The performance of the assembled single fuel cell was examined by an ElectroChem fuel cell test station (MTS-150). The evaluation of the effect of the catalyst loading was conducted using pure H_2 and O_2 as fuels. The CO resistance was then examined by feeding a syngas (CO/H_2, 20 ppm CO) to the cells.

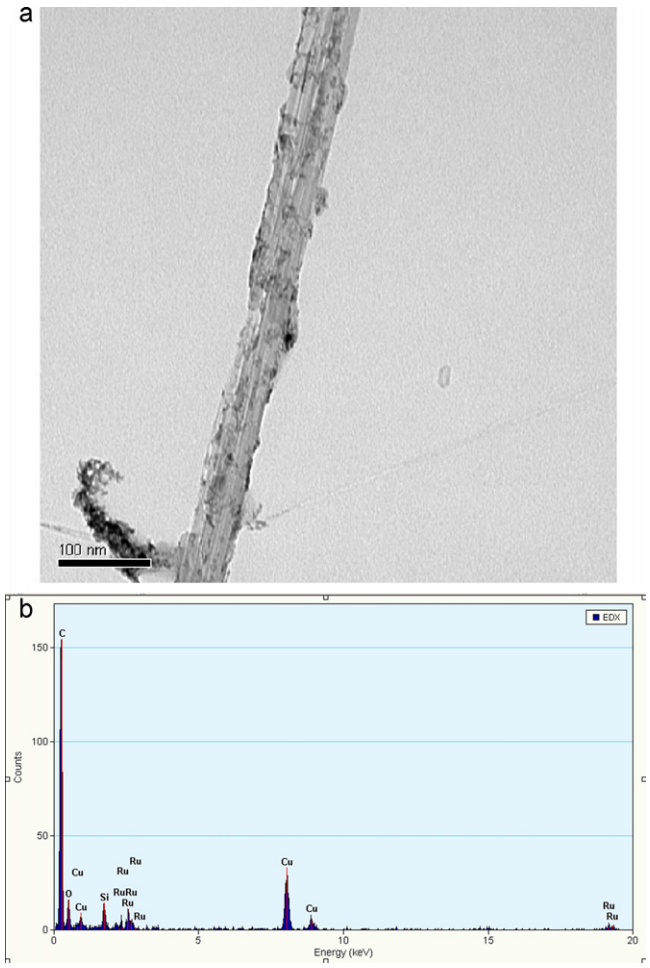

Fig. 2. The results of the first spontaneous deposition step. (a) TEM image and (b) EDX spectrum of Ru/CNTs.

4. Results and discussions

4.1. Electrochemical performance

The morphologies and microstructures of the prepared catalysts were examined by means of Transmission electron microscopy (TEM). The image of Ru nanoparticles/CNTs is presented in Fig. 2. After high-temperature treatment and a Ru deposition process, CNTs still maintain their original configurations and microstructures. The micrograph indicates that Ru black was deposited on the sidewalls of CNTs. An energy dispersive X-ray spectroscopy (EDS) analysis confirms the presence of Ru in the sample.

The deposition behavior of metal nanoparticles on the CNTs can be explained as the result of direct redox reactions between CNTs and metal ions. CNT has a reduction potential of about +0.5 V vs. SHE [33,34] and is able to reduce Ru^{3+} (Ru^{3+}/Ru, +0.68 V vs. SHE) [35] into a nanoparticle by a galvanic replacement reaction. This

Table 1
The contents of 3 different membrane electrode assemblies.

	Anode		Cathode	
	Material	Catalyst loading	Material	Catalyst loading
MEA 1	Pt/C (E-TEK)	0.4 mg Pt/cm^2	Pt/C (E-TEK)	0.4 mg Pt/cm^2
MEA 2	PtRu/CNTs	0.3 mg Pt/cm^2	Pt/C (E-TEK)	0.4 mg Pt/cm^2
MEA 3	PtRu/C (E-TEK)	0.3 mg Pt/cm^2	Pt/C (E-TEK)	0.4 mg Pt/cm^2

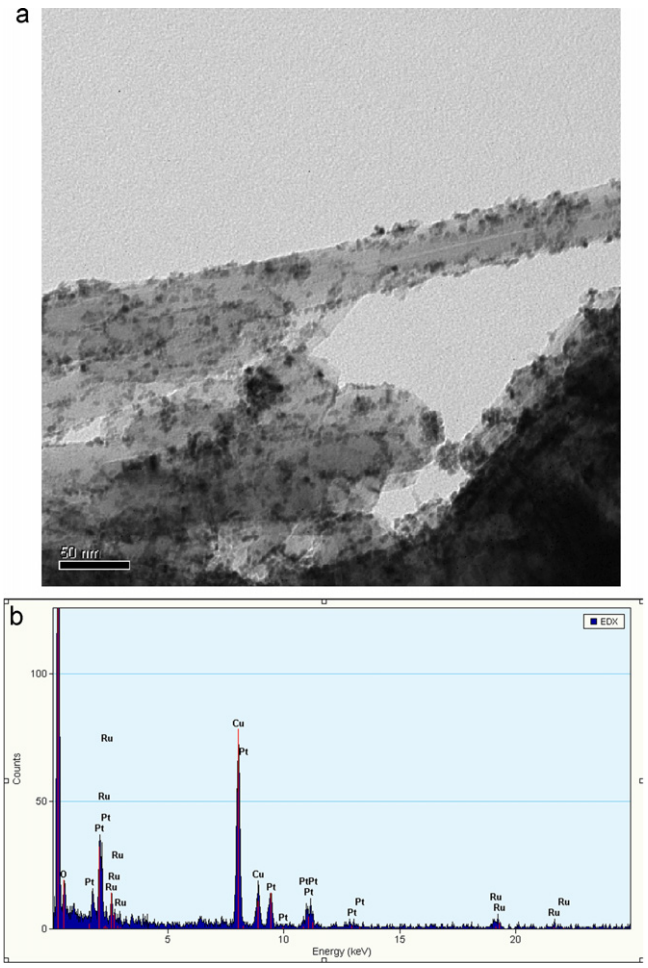

Fig. 3. The results of the second spontaneous deposition step. (a) TEM image shows an even distribution of Pt–Ru nanoparticles on CNTs and (b) EDX spectrum.

reaction takes place without the aid of any reducing agent or external energy. The electrons that form the valence band of CNTs will convert metal ions from the solution to metallic particles on the surface.

To deposit Pt on the prepared Ru/CNTs, a metallic Ru surface is required to let the spontaneous deposition occur. The surface of Ru/CNTs has to be reduced under H_2 gas at about 200 °C to remove RuOH species. Ru also provides an electron for reducing H_2PtCl_6 to Pt and changes Pt to an oxidation state [36]. The released chloride anions were discharged into the solution. After the spontaneous deposition process, undesired materials such as H_2SO_4, HCl and impurities need to be removed. The prepared electrocatalysts can be kept in pure water or in powder form after centrifuging and drying procedures.

Fig. 3 displays a TEM image of Pt–Ru/CNTs. It clearly shows that the Pt was uniformly dispersed on the Ru and on the sidewalls of CNTs. The two spontaneous deposition steps method successfully deposited Pt on the surface of Ru at the nanoscale level, which makes the whole catalyst available for the H_2 oxidation activity. Fig. 4 shows the morphology of three different catalysts. The home-made Pt–Ru/CNTs present a compatible catalyst distribution with commercial Pt/C and Pt–Ru/C (E-TEK, 20 wt.% of Pt and Ru).

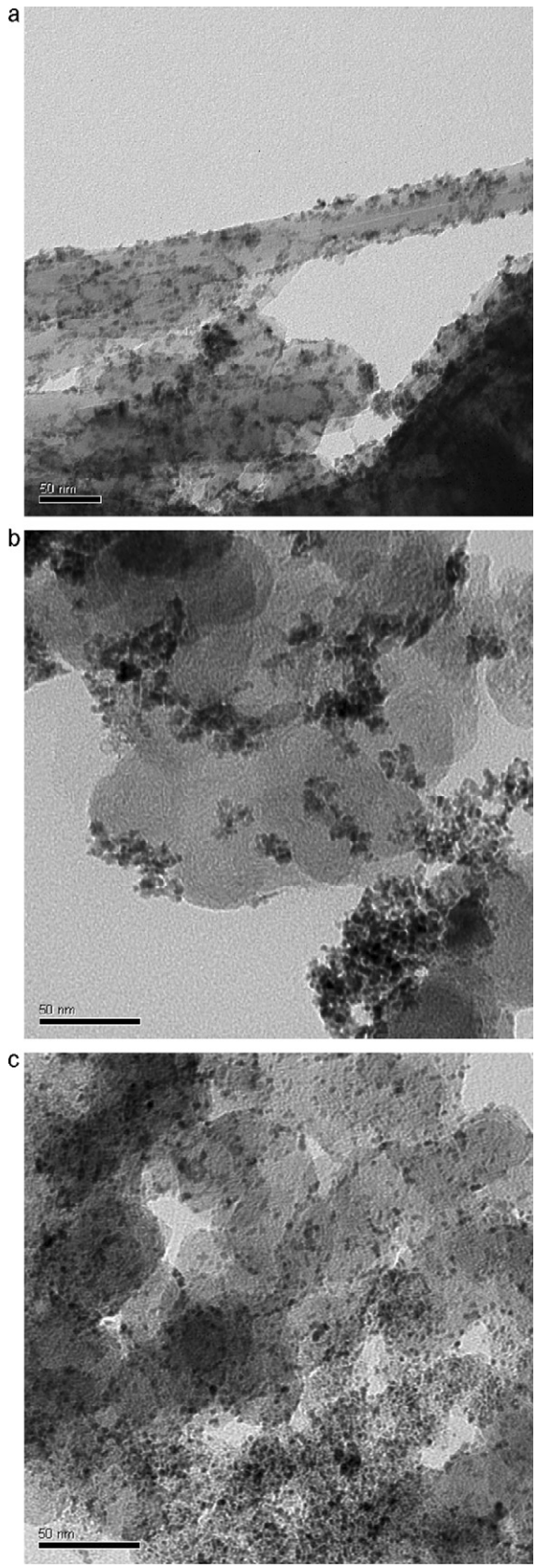

Fig. 4. The distribution conditions of metal particles. (a) Pt–Ru/CNTs, (b) Pt–Ru/C (E-TEK, 20 wt.% of Pt and Ru) and (c) Pt/C (E-TEK, 20 wt.% of Pt).

4.2. Voltammetry characterization

Fig. 5 displays the voltammetry curves of Pt/C (E-TEK, 20 wt.% of Pt), Pt–Ru/C (E-TEK, 20 wt.% of Pt and Ru) and Pt–Ru/CNTs in 1 M H_2SO_4. In the potential scanning range, the current density of

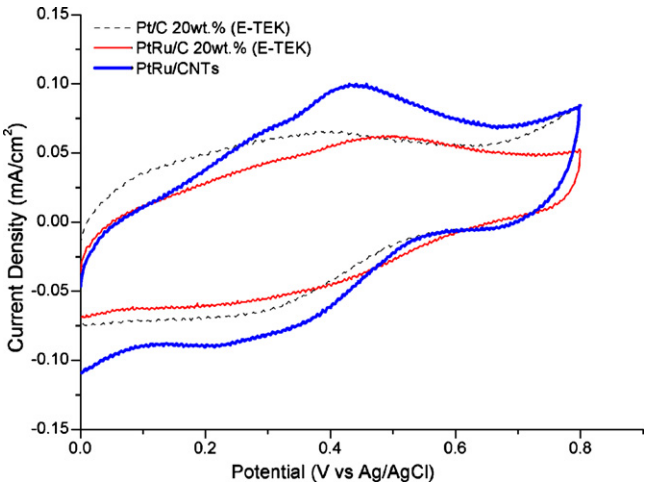

Fig. 5. Cyclic voltammetry tests for 3 different catalysts. Operation condition: scanning rate 20 mV s^{-1}, rotating disk at speed of 500 rpm.

Table 2
Performance of electrocatalysts in the CV experiments.

Catalyst	Performance	
	Current density (mA cm^{-2})	Mass activity (mA mg^{-1} catalyst)
Pt/C (E-TEK)	6.58×10^{-2}	1.89
PtRu/C (E-TEK)	6.25×10^{-2}	1.79
PtRu/CNTs	9.98×10^{-2}	5.43

Pt–Ru/CNTs at the oxidation peak is about 9.98×10^{-2} mA cm^{-2}, but the single metal catalyst (Pt/C) does not show the oxidation peak, which confirms that the effect of adding Ru to the electrocatalyst can increase the activity. For each 10 μl solution used in the test, there were 21.9 μg catalysts on the conductive support. The total weights of metal catalysts in Pt/C, Pt–Ru/C and Pt–Ru/CNTs are 4.38, 4.38 and 2.3 μg, respectively. In Table 2, the first column presents the highest current density for each catalyst during the oxidation process. The second column presents the calculated specific character. The Pt–Ru/CNTs catalyst exhibits a higher mass activity (5.43 mA mg^{-1}) for the H_2 reduction reaction than the commercial carbon-supported Pt (1.89 mA mg^{-1}) and Pt–Ru (1.79 mA mg^{-1}).

4.3. Fuel cell performance

The open circuit voltage of MEAs 1, 2 and 3 are 0.98, 0.94 and 0.94 V, respectively. When pure H_2 was supplied, as illustrated in Fig. 6, MEA 1 conducted a better fuel cell performance than MEA 2. This phenomenon can be ascribed to high Pt loading. The maximum power density of MEA 1 is 52 mW cm^{-2} at 140 mA cm^{-2}, but MEA 2 can only reach 43 mW cm^{-2} at 120 mA cm^{-2}.

Fig. 7 presents the cell potential vs. current density for two different types of catalysts fuelled by the syngas (CO/H_2, 20 ppm CO). The fuel cell with the Pt/C catalyst suffered a substantial perfor-

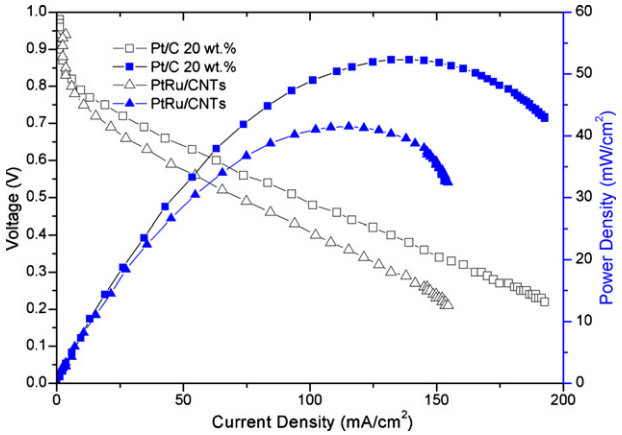

Fig. 6. Comparison of PEMFC performance with H_2 fuel. Catalyst type: (■) Pt/C (E-TEK, 20 wt.% of Pt), (▲) Pt–Ru/CNTs.

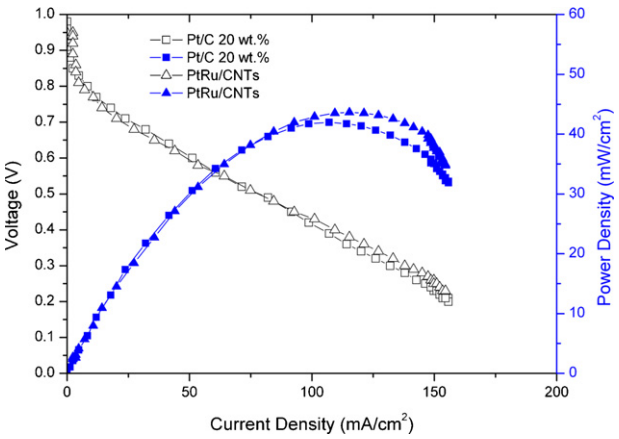

Fig. 7. Comparison of PEMFC performance with syngas (H_2/CO, 20 ppm CO) fuel. Catalyst type: (■) Pt/C (E-TEK, 20 wt.% of Pt), (▲) Pt–Ru/CNTs.

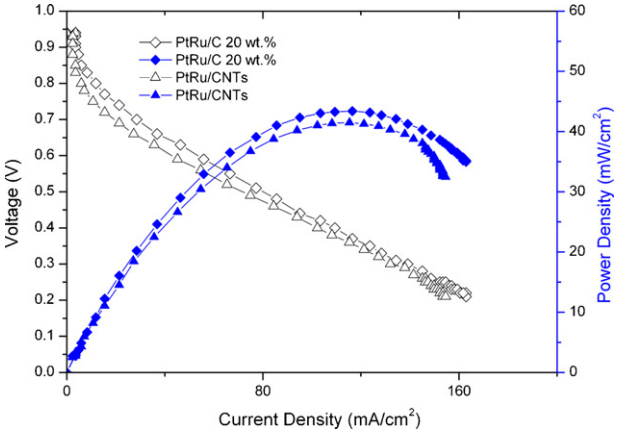

Fig. 8. As catalysts on the anode side of PEMFC, (♦) Pt–Ru/C (E-TEK, 20 wt.% of Pt and Ru) and (▲) Pt–Ru/CNTs perform a similar behavior with H_2 fuel.

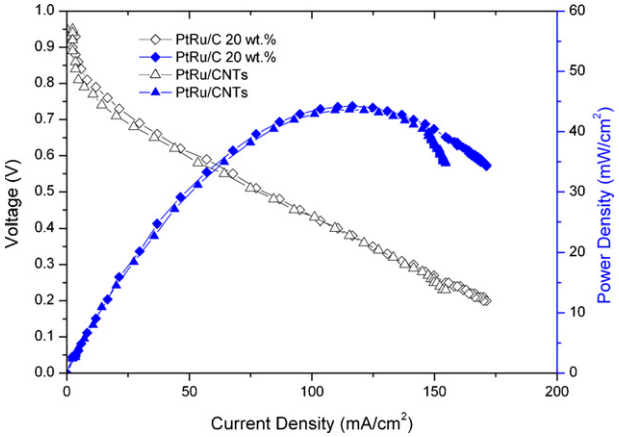

Fig. 9. As catalysts on the anode side of PEMFC, (♦) Pt–Ru/C (E-TEK, 20 wt.% of Pt and Ru) and (▲) Pt–Ru/CNTs perform a similar behavior with H_2/CO mixture (syngas) fuel.

mance decrease when CO was presented in the anode gas stream, but no voltage loss was found on the fuel cell using Pt–Ru/CNTs as the anode catalyst. In contrast to the single metal catalyst Pt/C, the presence of Ru in bimetal catalyst Pt–Ru/CNTs yields a significant improvement in CO tolerance.

As shown in Figs. 8–9, no matter whether pure H_2 or syngas was supplied as fuel, MEA 2 has similar performance to MEA 3. This result further confirms the contribution of Ru in preventing Pt from CO poisoning and the advantage of using CNTs as a support substrate for the catalyst.

5. Conclusions

A two-step spontaneous deposition method for preparing a bimetal catalyst with Pt and Ru on CNTs is proposed. The deposition of Ru nanoparticles on conductive support material, the CNTs, is made first. The new composite is then heated in a H_2 atmosphere at high temperature. The samples of Ru/CNTs are cooled down to ambient temperature and then placed in a solution containing Pt. After the second deposition process, the desired form of electrocatalyst Pt–Ru/CNTs is obtained. Higher Ru and Pt loadings can be made by repeating the spontaneous deposition procedure consecutively.

When Pt–Ru/CNTs are used as catalysts on the anode side of a PEM fuel cell, even with lower Pt loading (25% decrease) and 20 ppm, CO existed in the H_2 fuel, and the oxidization function of the catalyst was still maintained consistently. This type of electrocatalyst is suitable for fuel cells running on reformat, and is able to reduce the cost and improve the efficiency for SPFC.

References

[1] S. Gottesfeld, J. Pafford, J. Electrochem. Soc. 135 (10) (1988) 2651–2652.
[2] J. Larminie, A. Dicks, Fuel Cell System Explained, second ed., John Wiley & Sons, 2003, 406.
[3] E. Christoffersen, et al., J. Catal. 199 (1) (2001) 123–131.
[4] V.M. Schmidt, H.-F. Oetjen, J. Divisek, J. Electrochem. Soc. 144 (9) (1997) L237–L238.
[5] D.J. Ham, et al., Catal. Today 132 (1–4) (2008) 117–122.
[6] G. García, et al., Catal. Today 116 (3) (2006) 415–421.
[7] P. Liu, A. Logadottir, J.K. Nørskov, Electrochim. Acta 48 (25–26) (2003) 3731–3742.
[8] D.C. Papageorgopoulos, M. Keijzer, F.A. de Bruijn, Electrochim. Acta 48 (2) (2002) 197–204.
[9] J.-H. Wee, K.-Y. Lee, J. Power Sources 157 (1) (2006) 128–135.
[10] B. Moreno, et al., Combustion Synthesis and Electrochemical Characterisation of Pt–Ru–Ni Anode Electrocatalyst for PEMFC, vol. 76, Elsevier Science, 2007, 368–374.
[11] G. Lu, J.S. Cooper, P.J. McGinn, J. Power Sources 161 (1) (2006) 106–114.
[12] E. Antolini, Mater. Chem. Phys. 78 (3) (2003) 563–573.
[13] C. Lu, R.I. Masel, J. Phys. Chem. B 105 (40) (2001) 9793–9797.
[14] J Prabhuram, et al., Electrochim. Acta 52 (7) (2007) 2649–2656.
[15] M. Carmo, et al., J. Power Sources 142 (1–2) (2005) 169–176.
[16] K.Y. Lee, et al., Chem. Phys. Lett. 440 (4–6) (2007) 249–252.
[17] C.-F. Chi, M.-C. Yang, H.-S. Weng, J. Power Sources 193 (2) (2009) 462–469.
[18] E. Yoo, et al., J. Power Sources 180 (1) (2008) 221–226.
[19] K.-i. Tanaka, et al., Catal. Lett. 127 (1) (2009) 148–151.
[20] J. Wang, et al., J. Power Sources 176 (1) (2008) 128–131.
[21] R.C. Batra, et al., J. Solids and Structures 44 (23–24) (2007) 7577–7596.
[22] S.R. Brankovic, et al., J. Electroanal. Chem. 532 (1–2) (2002) 57–66.
[23] S. Manandhar, J.A. Kelber, Electrochim. Acta 52 (2007) 5010–5017.
[24] S.E. Huxter, G.A. Attard, Electrochem. Commun. 8 (11) (2006) 1806–1810.
[25] M.S. Zei, T. Lei, G. Ertl, Z. Phys. Chem. 217 (5) (2003) 447–458.
[26] H. Hoster, B. Richter, R.J. Behm, J. Phys. Chem. B 108(Compendex) (2004) 14780–14788.
[27] T.D. Jarvi, T.H. Madden, E.M. Stuve, Electrochem. Solid-State Lett. 2 (5) (1999) 224–227.
[28] E.R. Fachini, et al., Langmuir 19 (21) (2003) 8986–8993.
[29] D. Cao, S.H. Bergens, J. Electroanal. Chem. 533 (1–2) (2002) 91–100.
[30] I.G. Casella, M. Contursi, J. Electroanal. Chem. 606 (1) (2007) 24–32.
[31] F. Rodríguez-reinoso, Carbon 36 (3) (1998) 159–175.
[32] S.T. Kuk, A. Wieckowski, J. Power Sources 141 (1) (2005) 1–7.
[33] R. Memming, Photoinduced charge transfer processes at semiconductor electrodes and particles in electron transfer I, in: Topics in Current Chemistry, vol. 169, Springer, Berlin/Heidelberg, 1994, pp. 105–181.
[34] L. Qu, L. Dai, J. Am. Chem. Soc. 127 (31) (2005) 10806–10807.
[35] S.-H. Yoo, S. Park, Electrochim. Acta 53 (10) (2008) 3656–3662.
[36] N.S. Marinkovic, M.B. Vukmirovic, R.R. Adzic, Mod. Aspects Electrochem. 42 (2008) 1–52.